Characterization of PdO/Ce$_{0.8}$Y$_{0.2}$O$_{1.9}$ catalysts for carbon monoxide and methane oxidation

Meng-Fei Luo *, Zhi-Ying Pu, Mai He, Juan Jin, Ling-Yun Jin

Zhejiang Key Laboratory for Reactive Chemistry on Solid Surfaces, Institute of Physical Chemistry, Zhejiang Normal University, Jinhua 321004, China

Abstract

The Ce$_{0.8}$Y$_{0.2}$O$_{1.9}$ solid solution was prepared by nitrate sol–gel method, and a series of catalysts with different PdO loading were prepared using impregnation method. These catalysts were characterized by XRD, Raman, CO-TPR, CO$_2$- and O$_2$-TPD techniques. The PdO is highly dispersed on the surface of the solid solution when the loading is lower than 0.5 wt.%. As PdO loading increases to 2 wt.%, it begins to form the crystalline structure. CO$_2$-TPD profiles show that the CO adsorbed on highly dispersed PdO is more easily oxidized to CO$_2$ than that adsorbed on crystalline structure and O$_2$-TPD results indicate that it is more difficult to decompose for highly dispersed PdO than that for crystalline structure. CO-TPR profiles show that the highly dispersed PdO is easily reduced. Catalytic activities of these catalysts for CO and CH$_4$ oxidation indicate that both the highly dispersed and crystalline PdO are the active site for CO oxidation, while the crystalline structure is the active site for CH$_4$ oxidation.
© 2006 Elsevier B.V. All rights reserved.

Keywords: Ce$_{0.8}$Y$_{0.2}$O$_{1.9}$ solid solution; PdO; CO oxidation; CH$_4$ oxidation

1. Introduction

Ceria has been the subject of intense studies in recent years because of its broad applications in various fields, such as catalyst, polishing material and solid fuel cell [1–4]. In the field of catalysis, cerium oxide has been used as a promoter in three-way catalysts for removing exhaust gas due to its enhanced oxygen storage capacity (OSC) [5]. Also, it has been reported that CeO$_2$ and rare earth oxide can significantly promote the dispersion of noble metal or increase the thermal stability, thus favor catalytic activity [6,7], among which its foremost role is to act as an oxygen storage component [5,8].

The high OSC of CeO$_2$ is associated with its rich oxygen vacancies and easy shift between CeO$_2$ and Ce$_2$O$_3$ under corresponding conditions [9–11]. The capabilities of redox and thermal stability of cerium oxide under high temperature are strongly enhanced by introducing other elements into the CeO$_2$ lattice to form solid solution [12–14]. More recently, it was reported that the introduction of ZrO$_2$ in ceria lattice leads to remarkable improvement in thermal stability and oxygen storage capac-

ity [15–18]. With higher OSC, higher conversion efficiency and resistance to thermal aging are generally observed on the catalyst.

The catalytic oxidation at low temperature is an efficient way to convert CO to CO$_2$. The most efficient catalysts are noble metals, such as Au [19–25], Pt [26] and Pd [25,27], and their catalytic behaviors have been extensively investigated.

Methane is the main component of natural gas, and its structure is very different from that of CO. Moreover, methane is a hydrocarbon that is very difficult to be catalytically oxidized [28]. The catalytic oxidation of CH$_4$ has been studied as an alternative for environmental friendly combustion of gas fuels and this approach has no emission of deleterious gas [29]. It is well known that some noble metal catalysts such as Pt [30,31] and Pd [32–36] are most active for complete oxidation of the hydrocarbons.

In our previous work, a series of PdO/Ce$_x$Y$_{1-x}$O$_{1.5+0.5x}$ catalysts with different x have been studied and it was found that the PdO/Ce$_{0.8}$Y$_{0.2}$O$_{1.9}$ catalyst was the most active catalyst for the oxidation of methane [37]. With regard to the support, in this paper, the relationship between structure and activity of the PdO/Ce$_{0.8}$Y$_{0.2}$O$_{1.9}$ catalyst were further studied in order to confirm the active sites for CO and methane oxidation.

* Corresponding author. Fax: +86 579 2282595.
  E-mail address: mengfeiluo@zjnu.cn (M.-F. Luo).

2. Experimental

2.1. Preparation of catalysts

$Ce_{0.8}Y_{0.2}O_{1.9}$ mixed oxides was prepared by citrate sol–gel method which was described in our previous work [37]. The supported PdO catalysts were prepared by a conventional impregnation method using an aqueous solution of H_2PdCl_4 with a concentration of $8.85\,g\,L^{-1}$ (in Pd). The samples were dried at $120\,°C$ over night, and then calcined at $600\,°C$ in air for 4 h with a heating rate of $20\,°C\,min^{-1}$. The catalysts are denoted as $PdO/Ce_{0.8}Y_{0.2}O_{1.9}$, and the loading of Pd was 0.1, 0.5 and 2 wt.%, respectively.

2.2. Characterization

X-ray diffraction (XRD) patterns were collected on a Philips PW3040/60 automated powder diffractometer, using Cu Kα radiation ($\lambda = 0.1542\,nm$). The intensity data were collected at room temperature over a 2θ range of 20–75° with a step interval of 0.02°.

Raman spectra measurements were performed on a Renishaw RM 1000 with a confocal microprobe Raman system with an excitation wavelength of 632.8 nm.

With the aim of characterizing the desorption characteristics of these catalysts, the temperature-programmed desorption (TPD) of CO_2 and O_2 were performed on a home-made instrument. For CO_2-TPD measurement, a 100 mg of sample was located in a quartz micro-reactor and pre-treated in He ($30\,ml\,min^{-1}$) at $500\,°C$ for 0.5 h, then it was cooled down to room temperature. Then 10 consecutive pulses of 1 ml of CO were injected until the adsorption of CO was saturated. The samples were purged with He at the same temperature for 1 h to remove the physically adsorbed CO. Finally, the desorption step was conducted in flowing He from room temperature to $950\,°C$ with a constant rate of $20\,°C\,min^{-1}$. The procedure of temperature-programmed desorption of O_2 was similar to that of CO_2-TPD, except that the sample was pre-treated in O_2 with a flow rate of $30\,ml\,min^{-1}$. The signals of CO_2 and O_2 were analyzed using a Balzers Omnistar 200 mass spectrometer by monitoring $m/e = 44$ (for CO_2) and 32 (for O_2).

The reduction properties of the $PdO/Ce_{0.8}Y_{0.2}O_{1.9}$ catalysts were measured by CO-TPR (temperature-programmed reduction). About 50 mg of the catalyst was placed in a quartz tube without pretreatment, and then a reduction gas of 5% CO in Ar ($30\,ml\,min^{-1}$) was introduced. The reaction temperature rose from room temperature to $910\,°C$ with a constant rate of $20\,°C\,min^{-1}$. The amount of CO consumption and the signal of CO_2 were monitored by a Balzers Omnistar 200 mass spectrometer at $m/e = 44$.

The Pd dispersion of $PdO/Ce_{0.8}Y_{0.2}O_{1.9}$ catalysts was calculated from CO chemisorption uptakes measured by pulse chemisorption with a mass spectrometry (Omnistar TM) at $25\,°C$. The catalysts reduced by hydrogen were treated in a quartz microreactor with a H_2 stream of $8\,ml\,min^{-1}$. The temperature rose from 25 to $250\,°C$ with a constant rate of $5\,°C\,min^{-1}$ and maintained for 0.5 h, followed by a He purge of $30\,ml\,min^{-1}$ for 2 h at $25\,°C$.

2.3. Activity measurement for carbon monoxide and methane oxidation

The catalytic activity measurement was carried out in a fixed bed reactor. The catalysts were pressed to pellets, then crushed and sieved to 20–40 mesh. A 500 mg of catalyst was used for reaction. In both reactions, the total gas flow rate was $80\,ml\,min^{-1}$ and the reaction was stabilized for 1 h. In CO oxidation, the composition of inlet gas mixture was 3% CO, 3% O_2 in N_2. The inlet and outlet gas mixture was analyzed on a Agilent 6850 gas chromatograph equipped with a TCD detector attached with a HP PLOT column ($30\,m \times 0.32\,mm \times 12.0\,\mu m$). In methane oxidation, the inlet gas was 3% methane, 8% O_2 and 89% N_2. CH_4 was analyzed on a Shimadzu GC-14C gas chromatograph equipped with a FID detector attached with a supelcowax-10 column ($30\,m \times 0.25\,mm \times 0.25\,\mu m$).

3. Results and discussion

3.1. Structure characterization of $PdO/Ce_{0.8}Y_{0.2}O_{1.9}$ catalysts

Fig. 1 shows the XRD patterns of $PdO/Ce_{0.8}Y_{0.2}O_{1.9}$ catalysts with different Pd loadings calcined at $600\,°C$ for 4 h. From this figure, only cubic CeO_2 was observed. The lattice parameter of $PdO/Ce_{0.8}Y_{0.2}O_{1.9}$ catalysts is 0.5401 nm, which is smaller than that of pure CeO_2 (0.5410 nm) [38,39]. This is because the radius of Y^{3+} (0.092 nm) is smaller than that of Ce^{4+} (0.097 nm), which leads to the shrink of CeO_2 lattice when Ce^{4+} was partially substituted with Y^{3+}. This indicates that the $Ce_{0.8}Y_{0.2}O_{1.9}$ solid solution is formed in these catalysts. No characteristic diffrac-
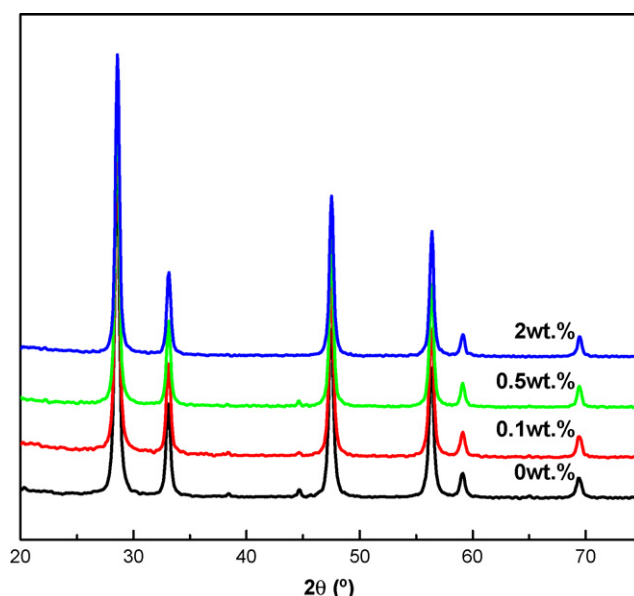
Fig. 1. XRD patterns of $PdO/Ce_{0.8}Y_{0.2}O_{1.9}$ catalysts.
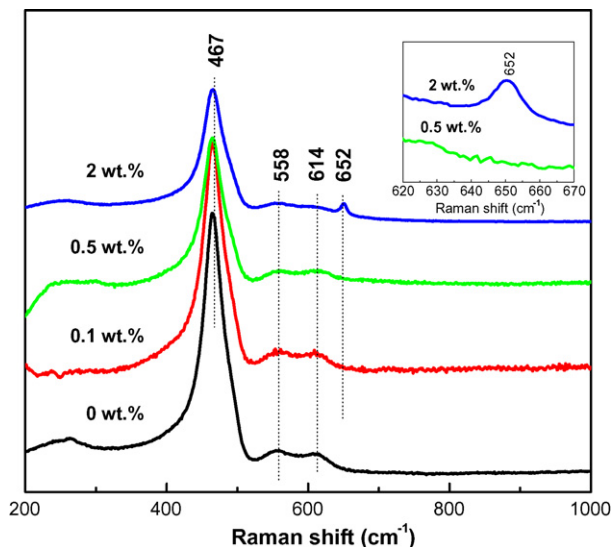
Fig. 2. Laser Raman spectra of $PdO/Ce_{0.8}Y_{0.2}O_{1.9}$ catalysts.
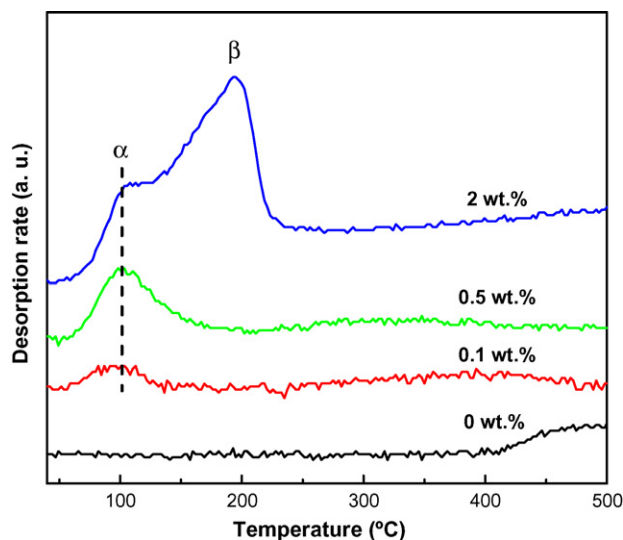
Fig. 3. The CO_2-TPD profiles of $PdO/Ce_{0.8}Y_{0.2}O_{1.9}$ catalysts.

tion peaks due to PdO (or Pd) was found for all the samples, which is probably due to the PdO (or Pd) is low or the PdO (or Pd) species that are highly dispersed on the surface of the $Ce_{0.8}Y_{0.2}O_{1.9}$ solid solution.

Fig. 2 shows the laser Raman spectra of $PdO/Ce_{0.8}Y_{0.2}O_{1.9}$ catalysts calcined at 600 °C for 4 h. The Raman band observed at 467 cm^{-1} is attributed to the $Ce_{0.8}Y_{0.2}O_{1.9}$ solid solution [37] and the characteristic peak of Y_2O_3 at 372 cm^{-1} was not observed [40,41]. This further proves the formation of $Ce_{0.8}Y_{0.2}O_{1.9}$ solid solution, which is consistent with the XRD results. The bands at 558 and 614 cm^{-1} are likely to be due to the formation of oxygen vacancies [42], which is also the evidence for the formation of solid solution.

Furthermore, when the Pd loading is lower than 0.5 wt.%, only Raman bands due to the solid solution were observed. As the Pd loading increases to 2%, a weak band at about 652 cm^{-1} was observed, which was ascribed to PdO [43]. The Raman signal of PdO (0.5%)/$Ce_{0.8}Y_{0.2}O_{1.9}$ catalyst was magnified as shown in the inset, however, the peak at 652 cm^{-1} ascribed to PdO was not observed, either. This indicates that the PdO species were highly dispersed at low loading. As the Pd loading increases up to 2%, the particles grow up to form crystalline PdO.

3.2. The CO_2-TPD and O_2-TPD characterizations of $PdO/Ce_{0.8}Y_{0.2}O_{1.9}$ catalysts

The CO_2-TPD profiles of $PdO/Ce_{0.8}Y_{0.2}O_{1.9}$ with different Pd loadings are shown in Fig. 3. It was found that no peaks due to CO desorption were observed (the figure is not shown in this paper). Only one CO_2 desorption peak at about 110 °C (α) was observed when Pd loading is low (0.1 and 0.5 wt.%). While at high loading (2 wt.%), a new CO_2 desorption peak at 195 °C (β) appears. From Raman results it could be seen that with low loading only highly dispersed PdO is existed on the surface of the solid solution, and it grows to crystalline structure as the loading increases. So the α and β peaks are likely to be ascribed to the

highly dispersed PdO and the crystalline structure, respectively. This indicates that the CO adsorbed on highly dispersed PdO is easier to be oxidized to CO_2 than that adsorbed on crystalline structure.

Fig. 4 shows the O_2-TPD profiles of $PdO/Ce_{0.8}Y_{0.2}O_{1.9}$ catalysts with different Pd loadings. In the range of 40–900 °C, no O_2 desorption peak was observed when the loading is 0.1 wt.%. While for the catalyst of 0.5% Pd loading, a peak with moderate intensity appears. As Pd loading increases to 2%, the intensity of O_2 desorption peak is augmented, furthermore, the temperature of O_2 desorption decreases remarkably. The desorption peak was attributed to the decomposition of PdO. This indicates that it is much more difficult to decompose for highly dispersed PdO than that for crystalline structure PdO, probably due to the strong interaction between highly dispersed PdO and the $Ce_{0.8}Y_{0.2}O_{1.9}$ solid solution.
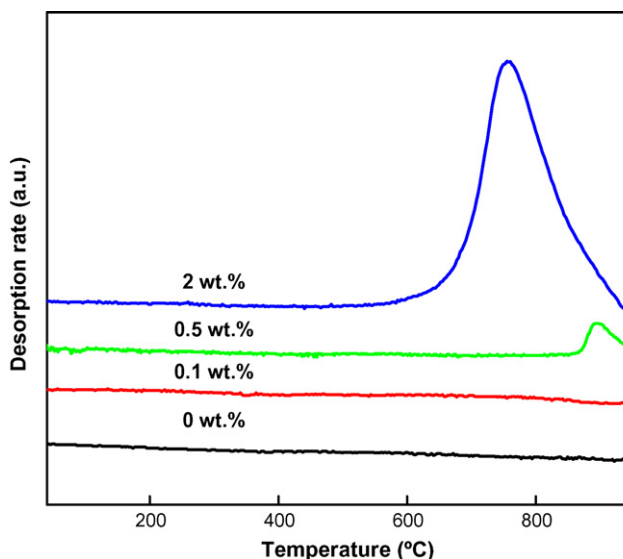
Fig. 4. The O_2-TPD profiles of $PdO/Ce_{0.8}Y_{0.2}O_{1.9}$ catalysts.

Fig. 5. The CO-TPR profiles of $PdO/Ce_{0.8}Y_{0.2}O_{1.9}$ catalysts.

Fig. 6. The catalytic activity of $PdO/Ce_{0.8}Y_{0.2}O_{1.9}$ catalysts for CO oxidation.
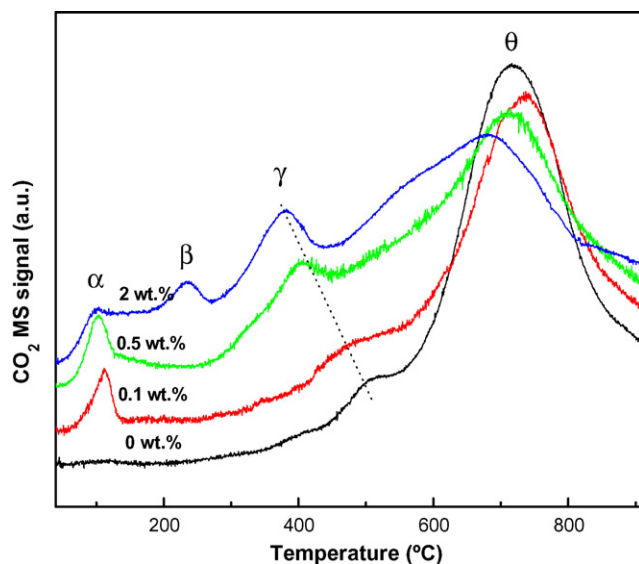
3.3. The CO-TPR characterization of $PdO/Ce_{0.8}Y_{0.2}O_{1.9}$ catalysts

The CO-TPR profiles of $PdO/Ce_{0.8}Y_{0.2}O_{1.9}$ catalysts with different Pd loadings are shown in Fig. 5. From Fig. 5, it can be seen that for the solid solution, no CO_2 signal was observed at low temperature (<400 °C), but two peaks appear at higher temperature region: a strong peak (θ) and a weak peak (γ). For the catalysts of 0.1 and 0.5 wt.% Pd, another peak at 105 °C (α) was observed besides the γ and θ peaks. The TPR profile of 2% Pd loading exhibits four peaks at 100 °C (α), 235 °C (β), 381 °C (γ), 682 °C (θ), respectively. It could be seen that the γ and θ peaks were present for all the catalysts, and the γ peak strongly shifted to lower temperature and its intensity strengthened as the PdO loading increased, while the intensity of θ peak declined with the increasing Pd loading. Therefore, it could be concluded that the γ peak is the reduction of surface oxygen on the solid solution and the θ peak is the reduction of bulk oxygen [44] and the reduction of surface sites is highly enhanced as PdO loading increases. Furthermore, the number of γ oxygen species increase and it get more active when the presence of PdO on the surface of solid solution. The α peak can be seen for all the cataysts, while the β peak could be observed only for the 2 wt.% Pd loading catalyst. Combined with the Raman results, it is reasonable to conclude that the α peak is ascribed to the reduction of highly dispersed PdO and the β peak is due to the reduction of crystalline PdO.

3.4. Catalytic activity for CO and CH₄ oxidation

Fig. 6 shows the catalytic activity of $PdO/Ce_{0.8}Y_{0.2}O_{1.9}$ for CO oxidation with various Pd loadings. None of these catalysts was pretreated before the reaction .The reaction was kept at each temperature for about 1 h to achieve steady activity. The T_{90} (the temperature when the conversion is 90%) for $PdO/Ce_{0.8}Y_{0.2}O_{1.9}$ catalysts with 0, 0.1, 0.5 and 2 wt.% Pd loadings are 300, 200,
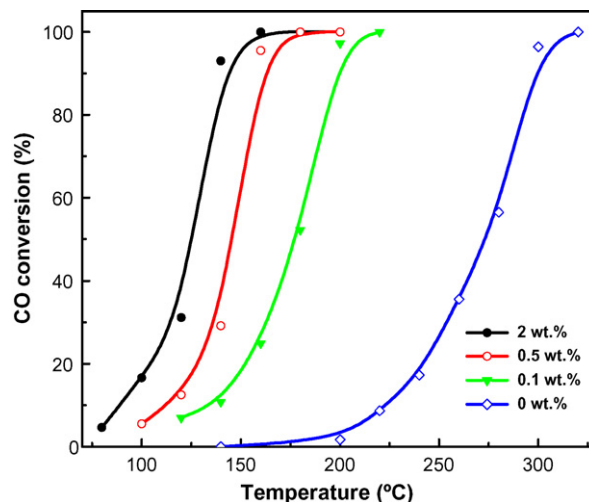
160 and 140 °C, respectively. It can be seen that the presence of a small amount of Pd can significantly enhance the catalytic activity.

Fig. 7 shows that the catalytic activities for CH_4 oxidation with $PdO/Ce_{0.8}Y_{0.2}O_{1.9}$ catalysts. From Fig. 7, it can be seen that the T_{90} for $PdO/Ce_{0.8}Y_{0.2}O_{1.9}$ catalysts with 0, 0.1, 0.5 and 2 wt.% Pd loadings are 580, 580, 580 and 500 °C, respectively. It implies that with low Pd loading (0.1 and 0.5 wt.%), the contribution of Pd species to the activity was limited. When the loading increases to 2 wt.%, the activity was enhanced.

In order to clarify the active site for CO and CH_4 oxidation, turnover frequency (TOF) [26] for CO and CH_4 oxidation over the catalysts were calculated based on Pd dispersion results and are listed in Table 1. The dispersion of PdO for 0.1, 0.5, 2 wt.% catalysts are 97.8%, 27.0% and 7.7%, respectively. The TOFs were calculated by subtracting the activity of the support, so the TOFs indicate the intrinsic activity of the PdO species. Since the support was inactive for CO oxidation at 140 °C (Fig. 6), while for CH_4 oxidation at 460 °C, the catalysts with 0.1 and 0.5 wt.% Pd loading had same activities as the support (Fig. 7). Note that
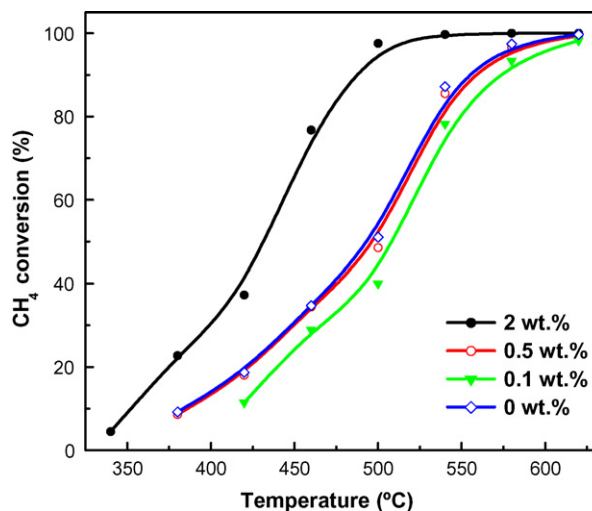
Fig. 7. The catalytic activity of $PdO/Ce_{0.8}Y_{0.2}O_{1.9}$ catalysts for CH₄ oxidation.

Table 1
Turnover frequency (s^{-1}) comparison between CO and CH_4 oxidation

PdO loading (wt.%)	Turnover frequency (s^{-1})	
	CO oxidation[a]	CH_4 oxidation[b]
0.1	0.045	0
0.5	0.083	0
2.0	0.230	0.104

[a] Calculated at 140 °C by subtracting the activity of support.
[b] Calculated at 460 °C by subtracting the activity of support.

the activity of 0.1 wt.% Pd loading catalyst was slightly lower than support for CH_4 oxidation, probably due to experimental error. From Table 1, it can be seen that for CO oxidation, the intrinsic activity was enhanced with increasing Pd loading. For CH_4 oxidation, the catalysts with 0.1 and 0.5 wt.% Pd loading have no contribution to the activity; while with 2 wt.% Pd loading the activity was improved.

The difference between the TOFs for CO and CH_4 oxidation clearly shows that the different active sites for the two reactions. For CO oxidation, both highly dispersed PdO species and crystalline PdO are active sites. For CH_4 oxidation, only crystalline PdO was responsible for the activity. However, it should be noticed that the highly dispersed PdO species could be easily reduced, as shown in CO-TPR results (Fig. 5), so during the reaction, the PdO sites could be partially reduced by CO and these reduced sites can activate both CO and O_2 reactants. Therefore, a mixed PdO_x phase could be present during CO oxidation. In contrast, the oxidic PdO could hardly be reduced by CH_4 even at high temperature, so it is more likely that the oxidic PdO species are the active sites for CH_4 oxidation.

4. Conclusions

PdO is highly dispersed on the surface of the $Ce_{0.8}Y_{0.2}O_{1.9}$ solid solution when the loading is low (≤ 0.5 wt.%), and it begins to form the large crystalline structure when the Pd loading increases to 2 wt.%. CO-TPR results reveal that highly dispersed PdO species are present on low Pd loading catalysts (0.1 and 0.5 wt.%), while on the high Pd loading catalyst (2 wt.%) there is a mixture of highly dispersed PdO and crystalline PdO. By comparing the turnover frequency of CO and CH_4 oxidation, it could be concluded that both the highly dispersed PdO and the crystalline structure PdO are the active sites for the reaction of CO oxidation, while the crystalline structure PdO is the active site for CH_4 oxidation.

Acknowledgement

References

[1] H.-M. Yang, C.-H. Huang, A.-D. Tang, Mater. Res. Bull. 40 (2005) 1690.
[2] B. -Tang, L.-H. Zhuo, J.-C. Ge, G.-l. Wang, Z.-Q. Shi, J.-Y. Niu, Chem. Commun. (2005) 3565.
[3] T.X.T. Sayle, S.C. Parker, D.C. Sayle, Chem. Commun. (2004) 2438.
[4] Z. Wang, X. Feng, J. Phys. Chem. B 107 (2003) 13563.
[5] H. Shinjoh, J. Alloy. Compd. 408-412 (2006) 1061.
[6] J. Guzman, A. Corma, Chem. Commun. (2005) 743.
[7] S. Carrettin, P. Concepcion, A. Corma, J.M.L. Nieto, V.F. Puntes, Angew. Chem. 116 (2004) 2592.
[8] L.-H. Xiao, K.-P. Sun, X.-L. Xu, X.-N. Li, Catal. Commun. 6 (2005) 796.
[9] A.K. Sinha, K. Suzuki, J. Phys. Chem. B 109 (2005) 1708.
[10] A. Trovarelli, S. Colussi, C. Leitenburg, G. Dolcetti, J. Alloy. Compd. 374 (2004) 387.
[11] G. Balducci, M.S. Islam, J. Kašpar, P. Fornasiero, M. Graziani, Chem. Mater. 12 (2000) 677.
[12] P. Fornasiero, J. Kaspar, M. Graziani, J. Catal. 167 (1997) 576.
[13] R. Lin, Y.-J. Zhong, M.-F. Luo, W.-P. Liu, Indian J. Chem. A 40 (2001) 36.
[14] M. Alifanti, B. Baps, N. Blangenois, J. Naud, P. Grange, B. Delmon, Chem. Mater. 15 (2003) 395.
[15] J. Kaspar, P. Fornasiero, M. Graziani, Catal. Today 50 (1999) 285.
[16] B.M. Reddy, A. Khan, P. Lakshmanan, J. Phys. Chem. B 109 (2005) 3355.
[17] P. Fornasiero, J. Kašpar, M. Graziani, Appl. Catal. B 22 (1999) L11.
[18] E. Mamontov, T. Egami, R. Brezny, M. Koranne, S. Tyagi, J. Phys. Chem. B 104 (2000) 11110.
[19] P. Konova, A. Naydenov, C. Venkov, D. Mehandjiev, D. Andreeva, T. Tabakova, J. Mol. Catal. A 213 (2004) 235.
[20] F. Moreau, G.C. Bond, A.O. Taylor, Chem. Commun. (2004) 1642.
[21] W. Yan, B. Chen, S.M. Mahurin, S. Dai, S.H. Overbury, Chem. Commun. (2004) 1918.
[22] M.A. Centeno, K. Hadjiivanov, T. Venkov, H. Klimev, J.A. Odriozola, J. Mol. Catal. A 252 (2006) 142.
[23] M.S. Chen, D.W. Goodman, Science 306 (2004) 252.
[24] U.R. Pillai, S. Deevi, Appl. Catal. A 299 (2006) 266.
[25] G. Glaspell, L. Fuoco, M.S. El-Shall, J. Phy. Chem. B 109 (2005) 17350.
[26] A. Wootsch, C. Descorme, S. Rousselet, D. Duprez, C. Templier, Appl. Surf. Sci (2006) doi:10.1016/j.apsusc.2006.02.006.
[27] M. Faticanti, N. Cioffi, S.D. Rossi, N. Ditaranto, P. Porta, L. Sabbatini, T. Bleve-Zacheo, Appl. Catal. B 60 (2005) 73.
[28] L.S. Escandon, S. Ordonez, A. Vega, F.V. Diez, Chemosphere 58 (2005) 9.
[29] B.-H. Yue, R.-X. Zhou, Y.-J. Wang, X.-M. zheng, J. Mol. Catal. A 238 (2005) 241.
[30] C. Bozo, N. Guilhaume, E. Garbowski, M. Primet, Catal. Today 59 (2000) 33.
[31] E. Marceau, H. Lauron-Pernot, M. Che, J. Catal. 197 (2001) 394.
[32] P. Reyes, A. Figueroa, G. Pecchi, J.L.G. Fierro, Catal. Today 62 (2000) 209.
[33] S. Yang, A. Maroto-Valiente, M. Benito-Gonzalez, I. Rodriguez-Ramos, A. Guerrero-Ruiz, Appl. Catal. B 28 (2000) 223.
[34] S. Guerrero, P. Araya, E. Wolf, Appl. Catal. A 298 (2006) 243.
[35] D. Ciuparu, L. Pfefferle, Appl. Catal. A 209 (2001) 415.
[36] L.F. Liotta, G. Deganello, J. Mol. Catal. A 204-205 (2003) 763.
[37] M.-F. Luo, W.-J. Shan, P.-L. Ying, J.-Q. Lu, C. Li, Stud. Surf. Sci. Catal. 138 (2001) 61.
[38] A. Bumajdad, M.I. Zaki, J. Eastoe, L. Pasupulety, Langmuir 20 (2004) 11223.
[39] M.-A. Einarsrud, T. Grande, I. Kaus, T. Mokkelbost, Chem. Mater. 16 (2004) 5489.
[40] M.Y. Jin-Ho Lee, K. Masato, Y. Masahiro, J. Phys. Chem. Solids 58 (1997) 1593.
[41] J.M. Calderon-Moreno, M. Yoshimura, Solid State Ionics 154/155 (2002) 125.
[42] J.R. McBride, K.C. Hass, B.D. Poindexter, et al., J. Appl. Phys. 76 (1994) 2435.
[43] S.C. Su, J.N. Carstens, A.T. Bell, J. Catal. 176 (1998) 125.
[44] S. Pengpanich, V. Meeyoo, T. Rirksomboon, K. Bunyakiat, Appl. Catal. A 234 (2002) 221.